Indonesian Journal of Electrical Engineering and Computer Science
Vol. 36, No. 2, November 2024, pp. 793~799
ISSN: 2502-4752, DOI: 10.11591/ijeecs.v36.i2.pp793-799

Research on the using of ZnO nanostructures to increase the white light-emitting diodes optics effectiveness

Phan Xuan Le, Pham Hong Cong
Faculty of Electrical Engineering Technology, Industrial University of Ho Chi Minh City, Ho Chi Minh City, Vietnam

Article Info

Article history:

Received Feb 27, 2024
Revised Jul 24, 2024
Accepted Jul 29, 2024

Keywords:

Color quality
Mie-scattering theory
White light-emitting diodes
YAG:Ce3+
ZnO nanostructures

ABSTRACT

In conventional white light-emitting diodes (WLEDs), the combination of blue-LED chips with a yellow-phosphor type is the commonly employed method of production. However, this approach often results in low angular correlated color temperature (CCT) homogeneity. To address this issue, this research proposes the incorporation of ZnO nanostructures into WLED packages to enhance color homogeneity. The impacts of varying concentrations of ZnO nanoparticles on the morphologies, scattered energy, and CCT deviations in WLED packages are studied utilizing the Mie-scattering theory and MATLAB measurement techniques to analyze the scattering effects of ZnO nanoparticles. The scattering analysis reveals that the presence of ZnO nanoparticles significantly increases the scattered strength of WLEDs, especially with larger particles' radii, due to their strong scattering influence. Then, 1 μm is the selected size of the ZnO used in further tests. With different ZnO concentrations (2-50 wt.%) in the phosphor layer, the CCT deviation holds an inverse proportion to the luminous efficiency. Particularly, higher concentrations of ZnO nanoparticles reduce the CCT deviation, leading to improved color homogeneity, but a decline in lumen efficiency. The findings provide the basis of ZnO scattering performance, which can be utilized to explore potential ways for enhancing WLED's color uniformity and overall performance.

Corresponding Author:

Phan Xuan Le
Faculty of Electrical Engineering Technology, Industrial University of Ho Chi Minh City
No. 12 Nguyen Van Bao Street, Ho Chi Minh City, Vietnam
Email: phanxuanle@iuh.edu.vn

1. INTRODUCTION

The use of light-emitting diodes (LEDs) as a promising generation solid-state illumination system has been demonstrated and will likely be used as an alternative to traditional fluorescent and incandescent lighting sources, by reason of they have remarkable characteristics such as durability, excellent performance, budget savings, and environmental friendliness [1]-[4]. Freely distributing the Ce^{3+}-doped $Y_3Al_5O_{12}$ (YAG:Ce) with yellow emission over to blue-LED chips [5], [6] is one of the most familiar techniques of white LED (WLED) manufacturing. However, the angle-associated hue heat obtained using this approach is of not good condition, and the yellow-ring issue, which is detrimental to WLED lighting output, also happens [7]-[9]. Authors recommended a variety of solutions to these issues, including conformal-phosphor structure [10], outer covering phosphor film adjustment [11], lens configuration [12], and WLED packet configuration optimization [13], [14]. While these approaches have been shown to improve CCT homogeneity, their manufacturing faces numerous challenges and they are often costly to be used in large scale manufacturing. WLED producers should also formulate a process that is easier and less costly to fabricate while also achieving high CCT homogeneity.

Diffuser-loaded encapsulation is currently a hopeful approach for improving the color consistency of WLEDs since it is able to meet the criteria of cost-saving and uncomplicated manufacture. WLED packets with diffuser bases containing metal oxides diffusional particles including TiO_2, SiO_2, and ZrO_2 have been evolved using this principle [15]-[18]. For instances, the ZrO_2 particle was incorporated with a diameter of 300 nm into the distant phosphor configuration, resulting in a decline in CCT difference by 580 K within ±70° viewing angle. Besides, the TiO_2 diffusers (320 nm) added to encapsulation or phosphor sheets resulted in decreased CCT deviations when increasing the doping concentrations. The influence of these diffusional particles on the CCT homogeneity of the WLED is obvious, but the influence of a diffusional substance or varying integrating amounts of related particles are the subject of the above studies. The effects of various diffuser material systems on WLED efficiency have not been analyzed in detail [5], [19], [20]. Furthermore, since there are not sufficient experiments that provide comprehensive content and detailed guidelines on this subject, pointing out the best nanoparticles to improve the color caliber of WLEDs takes a long period.

The scattered influences of ZnO nanostructures have recently been acknowledged and also advantageous for WLED processing because it is inexpensive and simple to monitor morphologies and synthesize [21]-[24]. Furthermore, by modifying and managing the reaction conditions including duration, temperatures, precursor dosage, and so on, a variety of ZnO configurations can be obtained. ZnO has a refractive index of 2.0, which indicates it is among GaN (n=2.5) and air (n=1), meaning that ZnO nanostructures can be called a refractive index gradient layer. Besides, so many researchers have highlighted the advantages of introducing ZnO to the GaN WLEDs to improve lighting extraction [25]-[27]. Though these papers demonstrated an increase in lighting intensity, the improvement in uniformity of color distribution of WLED models with diffusers of ZnO particles is barely discussed. Thus, in this paper, we will discuss the effect of using ZnO particles on the lighting quality of the WLED products. Mie theory of particle-scattering and the MATLAB measurement technique are used to investigate the scattering effects of ZnO nanoparticles, as seen in section 2. The results show that the scattered strength of WLEDs is increased due to the large scattered influence of ZnO nanoparticles. Furthermore, various ZnO concentrations may be used to improve color homogeneity.

2. METHODS OF SCATTERING ANALYSIS

The ZnO nano-spheres scattering used in simulation are spherical. Here, Mie-scattering-based formulas were utilized to analyze scattering fators of sphereical ZnO partciles [28], [29]. The scattering simulation was then carried out with varying ZnO diameters using the MATLAB computing program and illustrated in figures below.

The ZnO spheres' scattering properties, including scatter factor ($\mu_{sca}(\lambda)$), diffusing process functions (S_1 and S_2), decreased scatter factor ($\delta_{sca}(\lambda)$), and scatter cross-section (C_{sca}), are all shown in this chapter. As previously stated, the illumination scatter influences when ZnO nanoparticles are introduced is calculated using Mie theory and the MATLAB device [16]-[18]. The following formulas are used to calculate ZnO scattering:

$$\mu_{sca}(\lambda) = \int N(r) C_{sca}(\lambda, r) dr \quad (1)$$

$$g(\lambda) = 2\pi \int \int_{-1}^{1} p\,(\theta, \lambda, r) f(r) \cos\theta \, d\cos\theta \, d\, r \quad (2)$$

$$\delta_{sca} = \mu_{sca}(1 - g) \quad (3)$$

$$S_1 = \sum_{n=1}^{\infty} \frac{2n+1}{n(n+1)} [a_n(x, m)\pi_n(\cos\theta) + b_n(x, m)\tau_n(\cos\theta)] \quad (4)$$

$$S_2 = \sum_{n=1}^{\infty} \frac{2n+1}{n(n+1)} [a_n(x, m)\tau_n(\cos\theta) + b_n(x, m)\pi_n(\cos\theta)] \quad (5)$$

where $N(r)$ represents the diffuser density distribution, and r indicates the particle's radius (nm). $g(\lambda)$ denotes the anisotropy factor, and $p(\theta,\lambda,r)$ shows the phase function with λ represents the wavelength of excited light, and θ represents the scatter angle. $f(r)$ means the ZnO's size distributional density in the phosphor sheet. x and m represent the size parameters and refractive indexes. a_n and b_n represent the even and odd expansion coefficients, respectively. $\pi_n(\cos\theta)$ and $\tau_n(\cos\theta)$ represent the angular-dependence factors.

As the 450 nm and 550 nm wavelengths are the two main light regions for generating white light, we monitored the scattering properties of the ZnO at 450 nm and 550 nm and demonstrated in the following figures. In Figures 1 and 2, the scattering coefficients and phase functions are illustrated, in which the diameters of ZnO particles are varied from 0.1 to 1 µm. The increasing in ZnO diameters lead to the larger scattering productivity, suggesting that the incident-light absorbing probability is likely to be improved.

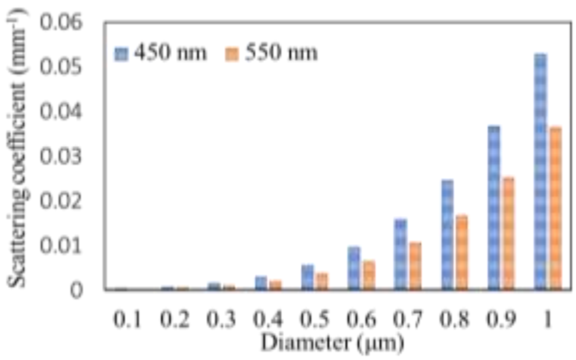

Figure 1. $\mu_{sca}(\lambda)$ with various particle sizes of ZnO spheres

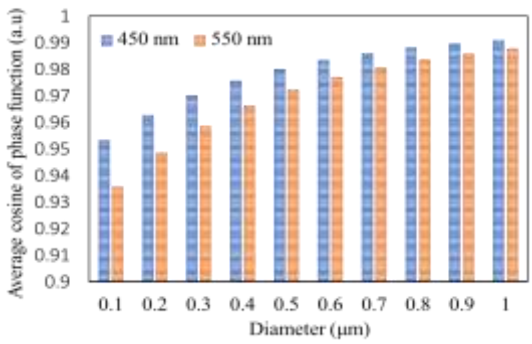

Figure 2. Phase functions with various particle sizes of ZnO spheres

Owing to the reflection process, the ZnO particle sizes can have a significant impact on scatter strength. The reduced scattering with various ZnO particle sizes is subsequently illustrated in Figure 3, and the scatter cross section in the same examination conditions is graphed in Figure 4. Similar to the scatter coeffucients and phase function, the larger ZnO diameter shows the stimulated scatter influence. It is evident from this that using large sizes of ZnO will homogenize the scatter strength distribution, but the backscattering influences can be greater if using along with high concentration in the phosphor film.

From the results shown in Figure 5, the scattering of light at 450 nm is always superior to that of 550 nm as can be shown. This proves that ZnO is suitable for use with improved LED color quality. Additionally, the bigger ZnO sphere diameter exhibits the larger scattering angle, which means the scattering probability of the light at LED packge's edges can be improved. Thus, the mixing of light rays is better for a higher overall uniformity of light-emission distribution. Conversely, the smaller ZnO sphere size leads to the narrower dispersion angle, which is probably advantageous for the strong and focus light emission. Therefore, the choice of balance between size and concentration becomes extremely important when applying ZnO.

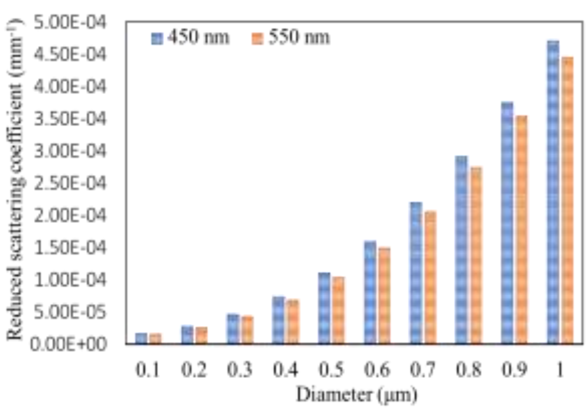

Figure 3. Decreased scattering coefficient with various particle sizes of ZnO spheres

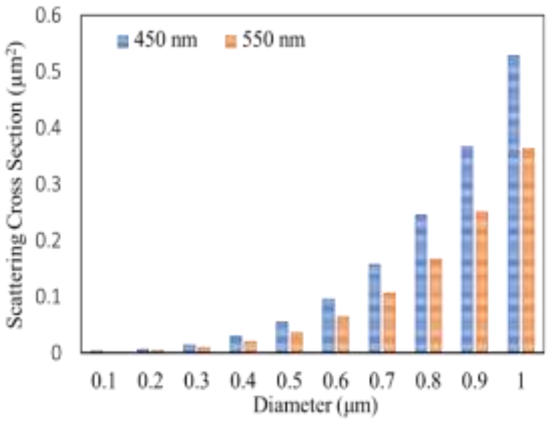

Figure 4. Scattering cross-section with various particle sizes of ZnO spheres

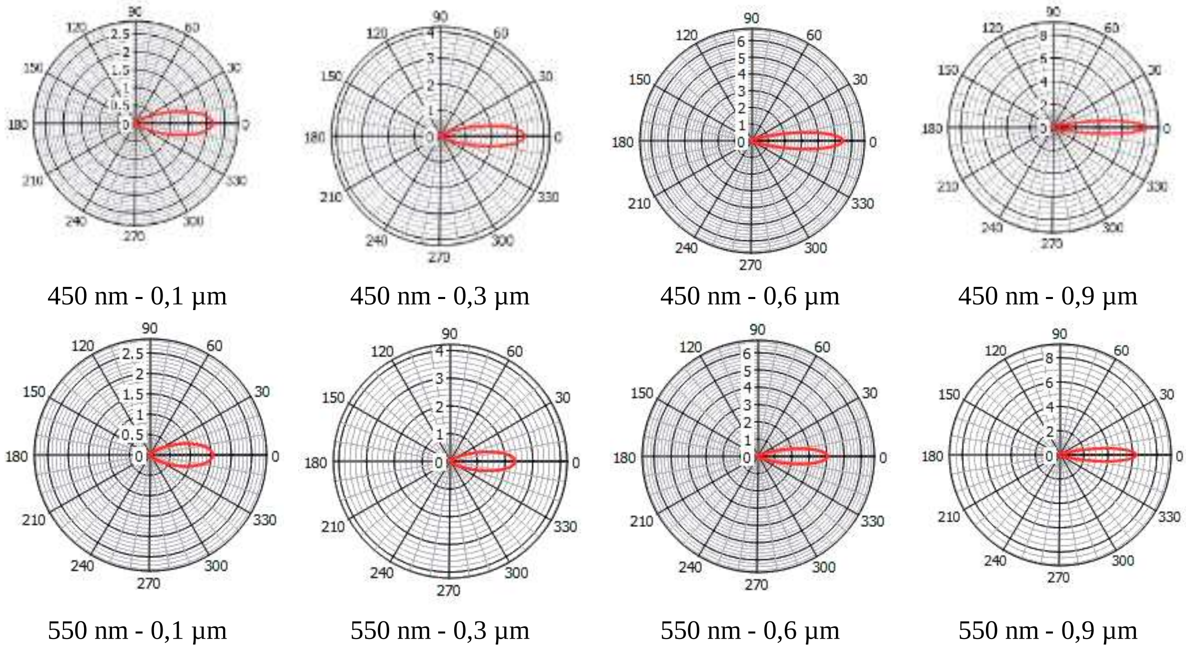

Figure 5. Angular scattering amplitudes with various particle sizes of ZnO spheres

3. COMPUTATION AND DISCUSSION

So as to check the measured outcomes of the influence of ZnO-doping films on WLEDs, the LightTools 8.1.0 program is used. The ZnO dopants with different concentrations are examined in order to include the most comprehensive study that can assist producers in using ZnO particles to improve their WLEDs. The diagrams of WLEDs used in this study as seen in Figure 6. The physically modelled WLED using multi-chip cluster can be seen in Figure 6(a) with specifications in Figure 6(b). Each component of a WLED product is carefully calibrated to ensure that the tested template is similar to the actual product. The LED reflector has a 2.1 mm depth, an 8-mm inside diameter, and a 10 mm outside diameter. The thickness of the ZnO/phosphor sheet covering the LED chips is 0.08 mm, as shown in Figure 6(c). Figure 6(d) is model provided by the LightTools simulation software [30], [31].

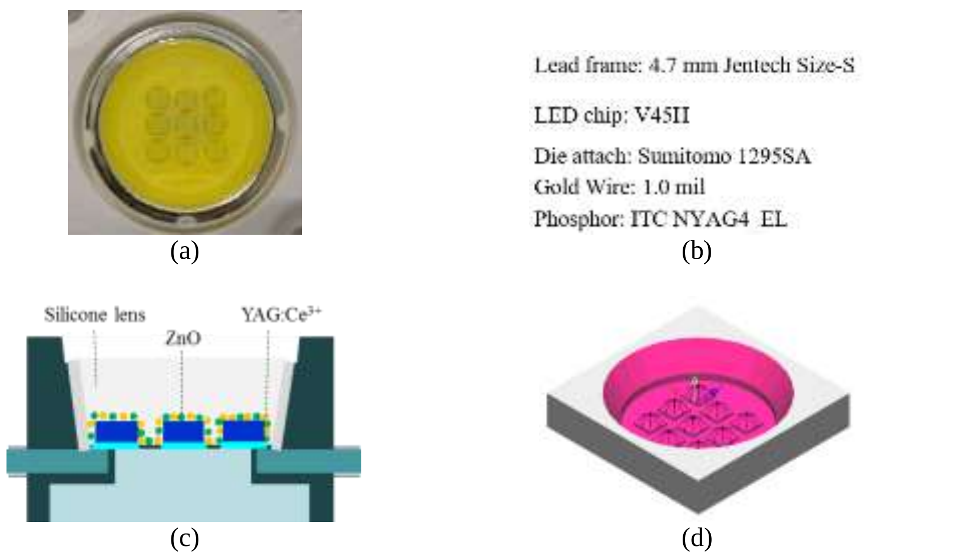

Figure 6. The diagrams of WLEDs: (a) picture of a WLED sample, (b) WLED specifications, (c) 2D illustration of a WLED, and (d) the simulated WLED by LightTools

The quantities and shapes of ZnO nanoparticles have a significant influence on inner diffusing, as previously observed. This chapter will look at how the optic output of WLEDs varies when ZnO is used as a diffuser film. The aim of the studies is to look into the scatter effects of ZnO in the phosphor film on the dispensation of CCT, illumination strength, and lighting quality [32], [33]. In a typical WLED packet, the ZnO dosage of the encapsulating film is comparable to that of the yellow phosphor. The angle dependent CCT homogeneity can be determined by the maximal CCT minus the minimal CCT, while the lighting intensity homogeneity can be shown as the highest value of lighting intensity minus the least one, due to the outcomes of earlier studies. Aside from that, as seen in Figure 7, the angle range used to assess angle-dependence CCT uniformity and luminescent strength is ±70°. As can be interpreted from the figure's data, the deviating CCT levels (delta-CCT) declines when increasing the ZnO concentrations. The lowest delta-CCT is noticed when ZnO wt.% is ~18. Though higher concentration of ZnO, for example 46 wt%, gives larger delta CCT, the value is lower than that of the package with <18 wt% ZnO dopants.

Figure 8 shows the illumination flux as a function of ZnO nanoparticle concentration. The conventional WLED product without ZnO had a comparatively high luminescent intensity, but it had low efficiency. The illumination flux can be increased by using ZnO-doped layers. Nevertheless, as the ZnO's concentration raises, the illumination flux decreases as the transference decreases, as a result of increasing ZnO concentration. The concentrations of ZnO in the phosphor layer greatly impacts the scattering performance. With low doping concentrations, the number of ZnO grains is insufficient to have an influence on lighting rays, making it difficult to discern between the effects of various morphologies. When the concentration of scatter particles drops below a specific threshold, the scattering factor can be described in terms of particle cloud properties. According to the general principle of dispersion, the light energy dispersed per spatial unit volume is proportional to the single-particle scattering energy. Even so, as the dosage of ZnO particles rises, the scattered energy dispensation is becoming more homogeneous, but the backscattering can become greater, inducing the re-absorption effects. As a consequence, the scattered light is absorbed, causing the total lighting extraction efficiency to decrease [34], [35].

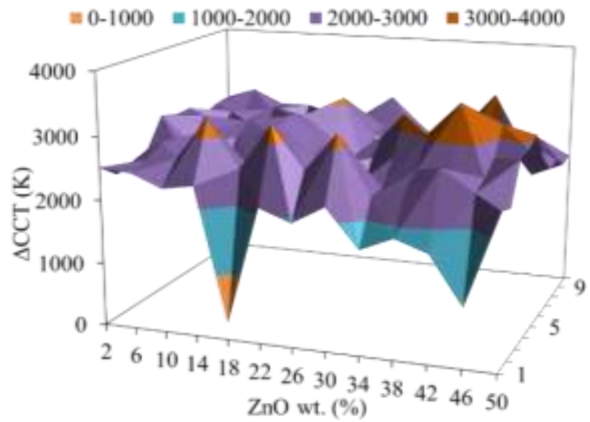

Figure 7. CCT deviations with various integrating amounts of ZnO spheres

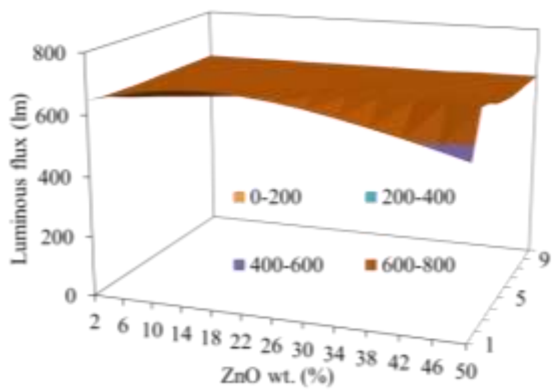

Figure 8. Illuminating beam with various integrating amounts of ZnO spheres

4. CONCLUSION

The study discusses the scattering properties of ZnO on the color homogeneity of the WLED. The color uniformity of the light output has been one of the critical concerns for high-power WLED devices. The ZnO with good scattering characteristics can be utilized as a scattering agent to induce the angular scattering performance of the conventional yellow YAG:Ce phosphor layer. The Mie-based scattering investigation for the ZnO spheres was performed with the varying particle's radius, aiming to determine the particle size for further examinations of ZnO influences. The obtained data showed that increasing the particle size of ZnO exhibited a stronger scattering performance, validating the ability of ZnO to stimulate the angular scattering of the phosphor layer. The appropriate ZnO diameter was selected at ~1 µm to be integrated into the phosphor layer. As the particle size was fixed, the concentration of ZnO was adjusted to obtain the research goal of improving angular color uniformity. The deviation of CCT was considered, which showed a noticeable decrease with increasing ZnO concentration, implying that the color homogeneity was enhanced. Specifically, the delta-CCT levels decreased when increasing the ZnO concentrations and bottomed out with 18 wt% of ZnO in the phosphor film. However, when increasing the ZnO concentration over a certain point, which is ~20 wt% in our examinations, the transmitting performance is reduced, resulting in a drop in luminescent performance. The reasonable concentrations for ZnO nanoparticles can be 18 wt% for the improvement of CCT uniformity and flux intensity. Such results demonstrated that using 1-µm ZnO at high concentrations of about 18-20 wt.% can contribute to achieving color uniformity with a minimum flux decline. Yet, the results are based on non-complex device simulation and with one phosphor material. Besides, another critical light property of the WLED – the color rendition – is not included in this study. Therefore, examining the performance of a more complex WLED structure with ZnO as a primary scattering particle or considering the effect of the ZnO diffuser layer on the color reproduction efficiency of the WLED can be appealing topics for future studies.

REFERENCES

[1] N. Li *et al.*, "High-efficiency solution-processed WOLEDs with very high color rendering index based on a macrospirocyclic oligomer matrix host," *Optical Materials Express*, vol. 8, no. 10, p. 3208, Sep. 2018, doi: 10.1364/ome.8.003208.

[2] N. D. Q. Anh, P. X. Le, and H.-Y. Lee, "Selection of a remote phosphor configuration to enhance the color quality of white LEDs," *Current Optics and Photonics*, vol. 3, no. 1, pp. 78–85, 2019.

[3] J. Zhang, L. Zhao, X. Bian, and G. Chen, " Ce 3+ /Mn 2+ -activated Ca 7 (PO 4) 2 (SiO 4) 2 : efficient luminescent materials for multifunctional applications," *Optics Express*, vol. 26, no. 18, p. A904, Aug. 2018, doi: 10.1364/oe.26.00a904.

[4] Y. J. Park *et al.*, "Development of high luminous efficacy red-emitting phosphor-in-glass for high-power LED lighting systems using our original low Tg and Ts glass," *Optics Letters*, vol. 44, no. 24, p. 6057, Dec. 2019, doi: 10.1364/ol.44.006057.

[5] W. Bao, M. Wei, and K. Xiao, "Investigating unique hues at different chroma levels with a smaller hue angle step," *Journal of the Optical Society of America A*, vol. 37, no. 4, p. 671, Mar. 2020, doi: 10.1364/josaa.383002.

[6] X. Li *et al.*, "Highly stable and tunable white luminescence from Ag-Eu^3+ co-doped fluoroborate glass phosphors combined with violet LED," *Optics Express*, vol. 26, no. 2, p. 1870, Jan. 2018, doi: 10.1364/oe.26.001870.

[7] K. Orzechowski, M. M. Sala-Tefelska, M. W. Sierakowski, T. R. Woliński, O. Strzeżysz, and P. Kula, "Optical properties of cubic blue phase liquid crystal in photonic microstructures," *Optics Express*, vol. 27, no. 10, p. 14270, May 2019, doi: 10.1364/oe.27.014270.

[8] W. Liu *et al.*, "Manipulation of LIPSS orientation on silicon surfaces using orthogonally polarized femtosecond laser double-pulse trains," *Optics Express*, vol. 27, no. 7, p. 9782, Mar. 2019, doi: 10.1364/oe.27.009782.

[9] P. Zhu, H. Zhu, G. C. Adhikari, and S. Thapa, "Spectral optimization of white light from hybrid metal halide perovskites," *OSA Continuum*, vol. 2, no. 6, p. 1880, May 2019, doi: 10.1364/osac.2.001880.

[10] C. McDonnell, E. Coyne, and G. M. O'Connor, "Grey-scale silicon diffractive optics for selective laser ablation of thin conductive films," *Applied Optics*, vol. 57, no. 24, p. 6966, Aug. 2018, doi: 10.1364/ao.57.006966.

[11] M. M. Magno-Canto, L. I. W. McKinna, B. J. Robson, and K. E. Fabricius, "Model for deriving benthic irradiance in the great barrier reef from MODIS satellite imagery," *Optics Express*, vol. 27, no. 20, p. A1350, Sep. 2019, doi: 10.1364/oe.27.0a1350.

[12] K. Matsushima and N. Sonobe, "Full-color digitized holography for large-scale holographic 3D imaging of physical and nonphysical objects," *Applied Optics*, vol. 57, no. 1, p. A150, Dec. 2018, doi: 10.1364/ao.57.00a150.

[13] Y.-L. Piao, M.-U. Erdenebat, K.-C. Kwon, S.-K. Gil, and N. Kim, "Chromatic-dispersion-corrected full-color holographic display using directional-view image scaling method," *Applied Optics*, vol. 58, no. 5, p. A120, Dec. 2019, doi: 10.1364/ao.58.00a120.

[14] J. Li *et al.*, "Double optical gating for generating high flux isolated attosecond pulses in the soft X-ray regime," *Optics Express*, vol. 27, no. 21, p. 30280, Oct. 2019, doi: 10.1364/oe.27.030280.

[15] M. Hu *et al.*, " Broadband emission of double perovskite Cs 2 Na 04 Ag 06 In 0995 Bi 0005 Cl 6 :Mn 2+ for single-phosphor white-light-emitting diodes," *Optics Letters*, vol. 44, no. 19, p. 4757, Sep. 2019, doi: 10.1364/ol.44.004757.

[16] L. He *et al.*, "Performance enhancement of AlGaN-based 365 nm ultraviolet light-emitting diodes with a band-engineering last quantum barrier," *Optics Letters*, vol. 43, no. 3, p. 515, Jan. 2018, doi: 10.1364/ol.43.000515.

[17] S. Jost, C. Cauwerts, and P. Avouac, "CIE 2017 color fidelity index Rf: a better index to predict perceived color difference?," *Journal of the Optical Society of America A*, vol. 35, no. 4, p. B202, Mar. 2018, doi: 10.1364/josaa.35.00b202.

[18] L. Li *et al.*, " 'Roller coaster'-like thermal evolution of the Er 3+ ion's red photoluminescence in CaWO 4 :Yb 3+ /Er 3+ phosphors," *Optics Letters*, vol. 44, no. 17, p. 4411, Aug. 2019, doi: 10.1364/ol.44.004411.

[19] R. Hirayama, H. Nakayama, A. Shiraki, T. Kakue, T. Shimobaba, and T. Ito, "Projection of multiple directional images on a volume structure with refractive surfaces," *Optics Express*, vol. 27, no. 20, p. 27637, Sep. 2019, doi: 10.1364/oe.27.027637.

[20] C. J. C. Smyth, S. Mirkhanov, A. H. Quarterman, and K. G. Wilcox, " 275 W/m 2 collection efficiency solar laser using a diffuse scattering cooling liquid," *Applied Optics*, vol. 57, no. 15, p. 4008, May 2018, doi: 10.1364/ao.57.004008.

[21] Y. Yang *et al.*, "Low complexity OFDM VLC system enabled by spatial summing modulation," *Optics Express*, vol. 27, no. 21, p. 30788, Oct. 2019, doi: 10.1364/oe.27.030788.
[22] S. P. Groth, A. G. Polimeridis, A. Tambova, and J. K. White, "Circulant preconditioning in the volume integral equation method for silicon photonics," *Journal of the Optical Society of America A*, vol. 36, no. 6, p. 1079, May 2019, doi: 10.1364/josaa.36.001079.
[23] L. Qin, X. Shi, and A. S. Leon, "Luminance calculation method accounting for mesopic vision and fog penetration ability," *Applied Optics*, vol. 59, no. 3, p. 683, Jan. 2020, doi: 10.1364/ao.59.000683.
[24] Z. Huang, Q. Liu, M. R. Pointer, W. Chen, Y. Liu, and Y. Wang, "Color quality evaluation of Chinese bronzeware in typical museum lighting," *Journal of the Optical Society of America A*, vol. 37, no. 4, p. A170, Mar. 2020, doi: 10.1364/josaa.381498.
[25] Y. Yu *et al.*, "Improving the color-rendering index of a tandem warm white organic light-emitting device by employing a simple fabrication process," *Optics Letters*, vol. 44, no. 4, p. 931, Feb. 2019, doi: 10.1364/ol.44.000931.
[26] Q. T. Vinh, P. Bodrogi, and T. Q. Khanh, "Preliminary measure for the characterization of the usefulness of light sources," *Optics Express*, vol. 26, no. 11, p. 14538, May 2018, doi: 10.1364/oe.26.014538.
[27] J. Cao, J. Zhang, and X. Li, "Upconversion luminescence of Ba3La, PO4.3:Yb3+-Er3+/Tm3," *Applied Optics*, vol. 57, no. 6, pp. 1345–1350, 2018.
[28] Q. Fu and W. Sun, "Mie theory for light scattering by a spherical particle in an absorbing medium," *Applied Optics*, vol. 40, no. 9, p. 1354, Mar. 2001, doi: 10.1364/ao.40.001354.
[29] I. W. Sudiarta and P. Chylek, "Mie scattering efficiency of a large spherical particle embedded in an absorbing medium," *Journal of Quantitative Spectroscopy and Radiative Transfer*, vol. 70, no. 4–6, pp. 709–714, Aug. 2001, doi: 10.1016/S0022-4073(01)00039-5.
[30] A.-M. D. Tran, N. D. Q. Anh, and N. T. P. Loan, "Enhancing light sources color homogeneity in high-power phosphor-based white LED using ZnO particles," *TELKOMNIKA (Telecommunication Computing Electronics and Control)*, vol. 18, no. 5, p. 2628, Oct. 2020, doi: 10.12928/telkomnika.v18i5.14198.
[31] T. C. Tran, N. D. Q. Anh, and N. T. P. Loan, "Excellent color quality of phosphor converted white light emitting diodes with remote phosphor geometry," *TELKOMNIKA (Telecommunication Computing Electronics and Control)*, vol. 18, no. 5, p. 2757, Oct. 2020, doi: 10.12928/telkomnika.v18i5.13575.
[32] N. T. P. Loan and N. D. Q. Anh, "Y2O3:Ho3+ and ZnO:Bi3+: a selection for enhancing color quality and luminous flux of WLEDs," *International Journal of Electrical and Computer Engineering*, vol. 10, no. 5, p. 5162, Oct. 2020, doi: 10.11591/ijece.v10i5.pp5162-5167.
[33] N. T. P. Loan and N. D. Q. Anh, "Utilizing CaCO3, CaF2, SiO2, and TiO2 particles to enhance color homogeneity and luminous flux of WLEDs," *International Journal of Electrical and Computer Engineering*, vol. 10, no. 5, p. 5175, Oct. 2020, doi: 10.11591/ijece.v10i5.pp5175-5182.
[34] G.-F. Luo, N. T. P. Loan, L. Van Tho, N. D. Q. Anh, and H.-Y. Lee, "Enhancement of color quality and luminous flux for remote-phosphor LEDs with red-emitting CaMgSi2O6:Eu2+,Mn2+," *Materials Science Poland*, vol. 38, no. 3, pp. 409–415, Sep. 2020, doi: 10.2478/msp-2020-0045.
[35] M. H. N. Thi, N. T. P. Loan, and N. D. Q. Anh, "The application of green YF3:Er3+,Yb3+ and red MgSr3Si2O8:Eu2+,Mn2+ layers to remote phosphor LED," *TELKOMNIKA (Telecommunication Computing Electronics and Control)*, vol. 18, no. 6, p. 3234, Dec. 2020, doi: 10.12928/telkomnika.v18i6.13827.

BIOGRAPHIES OF AUTHORS

Phan Xuan Le received the Ph.D. degree in Mechanical and Electrical Engineering from Kunming University of Science and Technology, Kunming City, Yunnan Province, China. Currently, He is a lecturer at the Faculty of Electrical Engineering Technology, Industrial University of Ho Chi Minh City, Ho Chi Minh City, Vietnam. His research interests are optoelectronics (LED), power transmission and automation equipment. He can be contacted at email: phanxuanle@iuh.edu.vn or phanxuanle.ts@gmail.com.

Pham Hong Cong received his MS in Electronic engineering from Danang University of Science and Technology, Vietnam, in 2010. He is a lecturer at the Faculty of Electrical Engineering Technology, Industrial University of Ho Chi Minh City, Ho Chi Minh City, Vietnam. His research interests are optoelectronics (LED), power transmission and automation equipment. He can be contacted at email: phamhongcong@iuh.edu.vn.